Frontiers in Health Informatics
ISSN-Online: 2676-7104
www.healthinformaticsjournal.com
2024;Vol. 13:Issue 7
OpenAccess

Silver and iron nanoparticles studies on *Torenia crustacea* (L.) Chamisso. & Schltendal.

S. Anusha and **Mary kensaV
*Research Scholar (Full-time), Reg. No: 22113152312008, PG Research Centre of Botany, S.T. Hindu College, Nagercoil-629002. Affiliated to Manonmaniam Sundaranar University, Tirunelveli, Tamil Nadu, India.
Email Id: anushaanusha9788932134@gmail.com
**PG Research Centre of Botany, S.T. Hindu College, Nagercoil -629002. Affiliated to Manonmaniam Sundaranar University, Tirunelveli, Tamil Nadu, India.
Email Id:surejkensa@gmail.com

Cite this paper as: S. Anusha and Mary kensaV (2024) Silver and iron nanoparticles studies on Torenia crustacea (L.) Chamisso. & Schltendal.. *Frontiers in Health Informatics*, *Vol.13, No.7, 1201-1216*

ABSTRACT

Nature has devised various processes for the synthesis of nano and micro length scaled inorganic materials which have contributed to the development of relatively new and largely unexplored area of research based on the biosynthesis of nanoparticles. Green synthesis of silver and iron nanoparticles was based on colour developed in the solution at the time of reaction and the colour intensity depends on peak in the UV-visible spectroscopy. FTIR analysis of silver nanoparticles confirms the presence of eight functional groups such as alkenes, aromatics, alkyl halides, esters, ketones, amides, aromatics and misc with frequency ranges (cm^{-1}). SEM analysis of *T. crustacea* brown coloured sample shows the presence of clustered spherical shaped, non-uniform distribution of silver nanoparticles and the TEM analysis enumerates many spherical shaped non-uniform distribution of silver nanopaticles of different sizes such as 7.98 nm, 12.34 nm, 11.87 nm, 13.56 nm and 15.92 nm having a mean size of about 16.09 nm lies in the nano range. FTIR analysis for iron nanoparticles of the ethanolic extract of the powdered whole plant of *T. crustacea* is used for identifying the functional groups of active components such as alkynes, alkanes, amides, misc, alkenes, carboxylic acids, aromatics and alkyl halides having the frequency range (cm^{-1}). SEM analysis having mostly clustered spherical shaped iron nanoparticles and the TEM images showed that spherical shaped iron nanoparticles of non-uniform distribution with mean size of about 16.07nm. Anti-microbial activity of the whole plant silver and iron coated extract of *T. crustacea* was performed by using five bacterial strains such as *Escherichia coli*, *Klebsiella pneumonia*, *Bacillus subtilis*, *Staphylococcus aureus*, *Lactobacillus acidophilus* and three fungal strains such as *Aspergillus niger*, *Aspergillus flavus* and *Pencillium notatum*.

KEY WORDS: FTIR, nanoparticles, SEM, TEM, *Torenia crustacea* etc.,

INTRODUCTION

Nanotechnology is emerging as an extensive interdisciplinary area of research all over the world for a few decades (Kandish and Chandrasekaran, 2021). Generally, nanoparticles are extremely small particles with their size ranging from 1 to 100 nm and exhibit completely new properties compared to the bulk materials (Jeong *et al*., 2005). It has gained significant attention due to the fabrication and application of nanopartices for several uses (Austin *et al*., 2014;

Connell *et al*., 2000) and possess novel properties and have chemical and biological properties (Ahmad *et al*., 2003). Besides, it has immense application in biomedical fields such as biomolecular detection, biosensors, anti-fungal, anti-bacterial and anti-angiogenetic agents (Salari *et al*., 2018).

The advent of nanotechnology profoundly transformed the pharmaceutical sciences and generally enhanced the diagnostics and treatment of various that threaten human life. Several metallic nanoparticles are extensively used as nanomedicines due to their potential therapeutic applications. Among these, silver nanoparticles are remarkable due to their unique chemical and physical properties (Vidyasagar *et al.,* 2023). The large surface area of silver nanoparticle is the primary factory that results in better anti-microbial activity due to strong interaction with microorganisms even at a lower concentration (Dhand *et al*., 2016).

Green synthesis of iron nanoparticles is a highly fascinating research area and has gained importance due to reliable, sustainable and eco-friendly protocol for synthesizing nanoparticles along with the easy availability of plant materials and their pharmacological significance (Vinod *et al*., 2023). Green synthesized iron nanoparticles display less toxicity and agglomeration with high stability due to effects of biomolecules present in biological extracts. Biological extracts overcome aggregation and oxidation of iron nanoparticles making the synthesis process as an eco-friendly, inexpensive and efficient technology (Rodrigues *et al*., 2013).

MATERIALS AND METHODS

Source of the plant material

The experimental plant, *T. crustacea,* (Plate 3.2) is collected from Kottaram, Agastheeswaram Taluk , Kanyakumari District, Tamil Nadu, India, Elevation about 460 meters (Mean Sea Level with 8.11 Latitude and 77.53 Longitude).

Characterization of silver nanoparticles

The optical property of the AgNPs was carried out by UV – visible absorption spectroscopy (Shimadzu – Bio Spec – Nano, Japan). A volume of 100µl of synthesized AgNPs were diluted with 900 µl of distilled water and subjected to spectral analysis in the wavelength range from 200-800 nm. The elemental composition of the synthesized AgNPs was confirmed by scanning electron microscopy. The Scanning electron microscopy spectroscopy (SEM) and Ultraviolet-visible spectroscopy were carrying out to confirmation of nano scale, uniformity and nano structure. The X-ray powder diffraction (XRD) was carried out using Rigaku X-ray diffractometer (Rigaku, Japan). The scanning was performed in the region of 2θ=30°–80° at 0.041°/min with a time constant of 2 seconds. The Fourier transform infrared spectrum (FTIR) of the AgNPs was obtained on a Bruker FTIR Spectrometer ALPHA II in the diffuse reflectance mode at a resolution of 4 cm-1 in KBr pellets. The FTIR spectrum was used to identify the functional groups in the plant extract responsible for the reduction of silver ions for the synthesis of silver nanoparticles (Sahayaraj *et al* ., 2011).

Characterization of iron nanoparticles

The changes in the reaction mixtures were observed visually and recorded. The sample was then spectrophotometrically examined in the UV-Vis range. The wavelength was scanned at 1 nm intervals from 200 to 700 nm. The instrument was turned on and given ten minutes to initialize. The sample solutions were placed in a quartz cuvette (1 cm), and the baseline was adjusted using ultra purified water as the baseline. In the wavelength range of 200 to 700 nm,

the spectra of extract, FeNPs, and ferric chloride solutions. FTIR system was used to make the measurements. The extract functional groups that may have played a role in the synthesis of iron microstructures were identified using FTIR scans of iron NPs. The transmission mode range of 400–4000 cm-1 was used for the FTIR analysis. TEM microscope with a 200 keV acceleration voltage was used to create the TEM images. The FeNP sample solutions were sonicated for 20 seconds in analytical grade methanol before being mounted on a carbon-coated copper grid with a mesh size of 200. The cleaned Teflon block was placed face-up on the treated grid, and 10 L of the NP sample solution was poured onto the grid and dried under an infrared lamp before the grid was loaded onto the microscope for measurements. The average particle size was calculated and recorded using FeNP samples randomly selected from TEM images. X-ray diffractometer was used to examine crystalline metallic iron NPs. The instrument used Cu Kα radiation at 45 kV and a monochromatic filter with a 20-80-degree wavelength range. Before being stacked in the cubes of the XRD equipment, the biosynthesized FeNPs were thoroughly dried to powder form (Thiyagarajan *et al*., 2018).

Anti-microbial activity

Test Organisms

The test microorganisms used for anti-bacterial analysis *Klebsiella pneumoniae*, *Bacillus subtilis*, *Staphylococcus aureus*, *Escherichia coli* and *Lactobacillus acidophilus* were purchased from Microbial Type Culture Collection and Gene Bank (MTCC) Chandigarh. The bacterial strains were maintained on Nutrient Agar (NA).

Nutrient Broth Preparation

Pure culture from the plate were inoculated into nutrient agar plate and sub cultured at 37ºC for 24 hr. Inoculum was prepared by aseptically adding the fresh culture into 2 ml of sterile 0.145 mol/L saline tube and the cell density was adjusted to 0.5 Mc Farland turbidity standard to yield a bacterial suspension of 1.5×10 8 cfu/ml. Standardized inoculum used for anti-bacterial test.

Anti-bacterial Test

The medium was prepared by dissolving 38 g of Mueller-Hinton Agar Medium (Hi Media) in 1000 ml of distilled water. The dissolved medium was autoclaved at 15 Lbs pressure at 121ºC for 15 min (pH 7.3). The autoclaved medium was cooled, mixed well and poured in to Petri plates (25 ml/plate). The plates were swabbed with pathogenic bacterial culture viz. *Klebsiella pneumoniae, Bacillus subtilis, Staphylococcus aureus, Escherichia coli* and *Lactobacillus acidophillus*. Finally, the sample loaded disc was then placed on the surface of Mueller-Hinton Agar medium. The standard drug Streptomycin 100 mg concentration disc was used for positive control and empty sterile disc was used for negative control. The plates were kept for incubation at 37°C for 24 hours. At the end of incubation, inhibition zones were examined around the disc (including disc) and measured with transparent ruler in millimetres (Kohner *et al*., 1994; Mathabe *et al*., 2006; Assam *et al*., 2010).

Anti-fungi Test (Bauer *et al*., 1966)

Anti-biotic susceptibility tests were determined by agar disc diffusion (Kirby-Bauer) method. Fungal strains such as *Aspergillus flavus, Aspergillus niger* and *Pencillium notatum* were swabbed using sterile cotton swabs on SDR agar plate. Upto 80 µl of each concentration of the extract respectively introduced into to the sterile discs (10 mm) using sterile pipettes. The standard drug Fluconazole 150 mg concentration was introduced in the sterile disc (10 mm) for

positive control and empty sterile disc was used for negative control. The disc was then placed on the surface of SDA medium and the compound was allowed to diffuse for 5 minutes and the plates were kept for incubation at 22°C for 48 hours. At the end of incubation, inhibition zones were examined around the disc and measured with transparent ruler in millimeters.

Synthesis of silver nanoparticles (Umoren *et al*., 2014)

300 ml of distilled water were added to 2.54 g of silver nitrate (0.05 M) and stirred to give nitrate solution. The solution was stirred with a magnetic stirrer for 5 minutes during the addition of 20 ml of whole plant extract and observed for colour change. The initial pale yellow colour of the mixture changed to dark brown after 72 hours indicating the reduction from Ag+ to Ag0. The resulting mixture was centrifuged at 4000 rpm for 20 minutes. The supernatant was discarded and the residues were oven dried at 70^0 C to afford the silver nanoparticles as a brownish powder.

Synthesis of iron nanoparticles (Makarov *et al*., 2014)

A simple conventional heating method was used in the synthesis of iron nanoparticles (FeNPs) by using plant extract. Plant extract was prepared by dissolving 2 gm of the sieved powder in 50 ml of deionized water and the resulting mixture kept on stirring for 3 hours by using the magnetic stirrer. The resulting solution was placed to stable for 1 hour and then filtered. 10 ml of 0.01 M $FeSO_4$ solution was stirred at 70°C and the plant extract (filtrate) was added after every interval of 5 minutes using 2 ml in each interval until the volume reach as 50 ml. The difference of temperature was noted after every interval of 5 minutes. The solution was placed to cool down and the product was parted by centrifugation (10,000 rpm) for 2 minutes. The product was dried in an oven at 50°C for 3 hours. The plant extract (filtrate) acts as reducing capping and stabilizing agent in iron nanoparticles synthesis.

RESULT AND DISCUSSION

Silver nanoparticles studies of the experimental plant

Green synthesis of silver nanoparticles was described based on colour developed in the solution at the time of reaction and the colour intensity itemized the bioreduction of silver particles during the inclusion of *T. crustacea* whole plant aqueous extract while, the formation of silver nanoparticles was perceived depends on peak in the UV-visible spectroscopy.

i. UV-visible spectroscopic analysis and XRD pattern of silver nanoparticles of the experimental plant

UV-visible spectroscopic analysis of *T. crustacea* whole plant extract exhibit a typical spectroscopic reaction at the wavelength of 427nm in which the initial pale yellow colour of the mixture changed to dark brown in colour. This validates the presence of silver nanoparticles present in *T. crustacea* and the X-ray diffraction pattern of silver nanoparticles at 2Ø values ranging from 20^0 to 60^0 shows nine major peaks and the synthesized silver nanoparticles are crystalline in nature of 4.90nm which are all clearly reported in the figure 1.

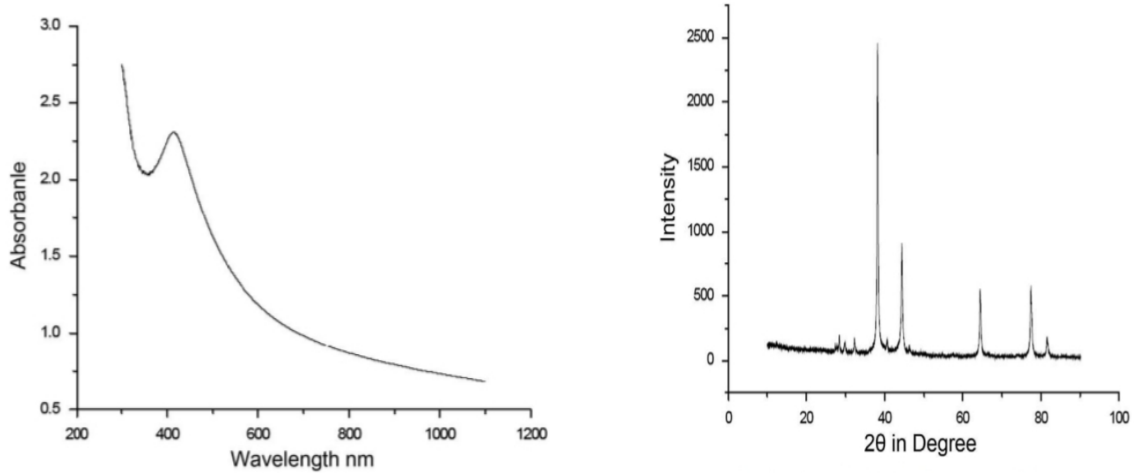

UV-visible spectrum **XRD spectrum**

Figure 1: Chromatogram for UV-visible and XRD spectroscopic analysis showing silver nanoparticles.

ii. FTIR analysis for silver nanoparticles

FTIR analysis for silver nanoparticles of the ethanolic extract of powdered whole plant of *T. crustacea* is used to recognize the functional groups of active compounds based on the peak value in the region of infrared radiation.

Table 1: FTIR analysis of the ethanolic extract of powdered whole plant of *T. crustacea* (L.) Cham. & Schltdl. for silver nanoparticles.

SI. N0.	Wave length	Functional groups	Structure
1	2358.87	Misc.	Si-H silane
2	1552.14	Akenes	4-ring
3	1267.78	Misc.	P=O phosphoramide
4	798.45	Aromatics	Meta-disub
5	730.65	Aromatics	1,3,5-trisub
6	653.98	Alkyl halides	R-Br
7	623.19	Alkyl halides	R-Br
8	1773.18	Esters	RCOOR’5-ring

9	1751.26	Ketones	R2CO 5-ring
10	1531.78	Amides	RCONHR
11	759.13	Aromatics	Ortho-disub
12	687.49	Aromatics	1,3,5-trisub
13	1006.73	Misc.	P-OR esters

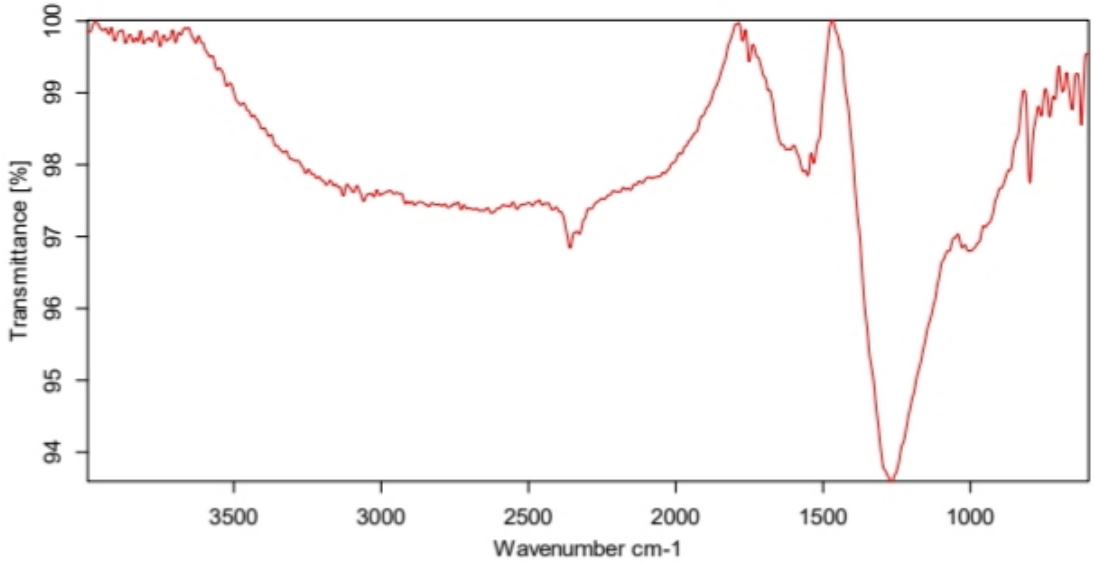

Figure 2: Chromatogram for FTIR analysis of the ethanolic extract of powdered whole plant of *T. crustacea* (L.) Cham. & Schltdl. for silver nanoparticles.

FTIR analysis confirms the presence of eight functional groups such as alkenes, aromatics, alkyl halides, esters, ketones, amides, aromatics and misc with frequency ranges (cm^{-1}) such as 2358.87, 1552.14, 1267.78, 798.45, 730.65, 653.98, 623.19, 1773.18, 1751.26, 1531.78, 759.13, 687.49 and 1006.73 respectively which are clearly mentioned in the table 1& figure 2.

iii. SEM and TEM analysis

SEM analysis for silver nanoparticles of the whole plant ethanolic extract of *T. crustacea* of the brown colour sample shows the presence of silver nanoparticles and well dispersed nanoparticles could be seen in the sample treated with silver nitate forming a cluster of spherical shaped, non-uniform distribution of silver nanoparticles and the TEM analysis enumerates many spherical shaped non-uniform distribution of silver nanopaticles of different sizes such as 7.98 nm, 12.34 nm, 11.87 nm, 13.56 nm and 15.92 nm having a mean size of about 16.09 nm lies in the nano range as clearly visible in the plate 1.

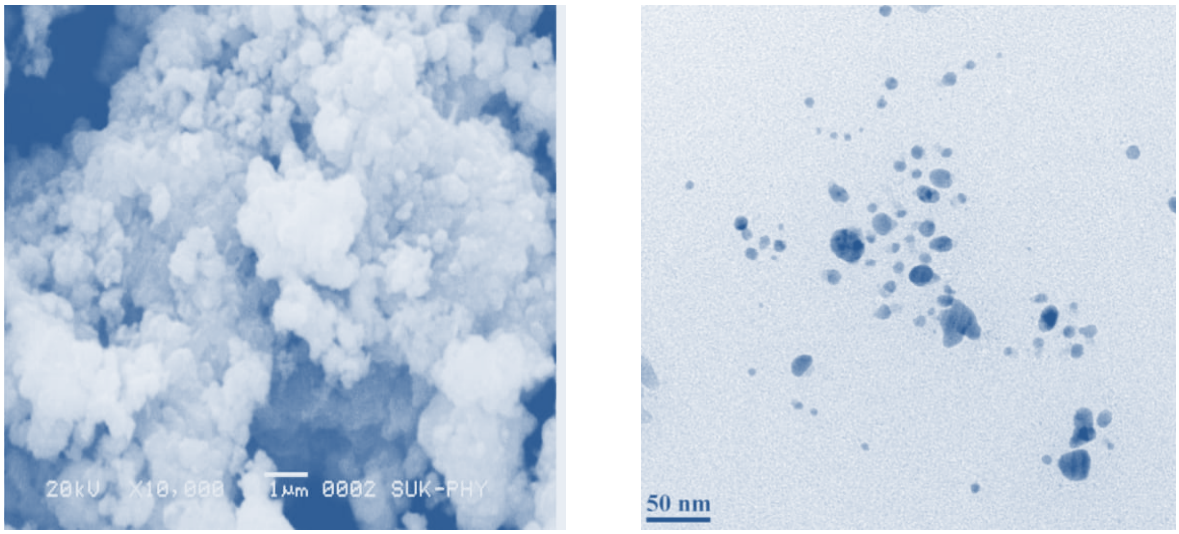

A) SEM **B) TEM**

Plate 1: SEM and TEM image showing silver nanoparticles of *T. crustacea*

Iron nanoparticles studies of the experimental plant

Green synthesis of iron nanoparticles of the whole plant aqueous extract of *T. crustacea* was studied based on the peak in the UV-visible spectroscopic analysis.

i. UV- visible spectroscopic analysis and XRD pattern of iron nanoparticles

UV-visible spectroscopic analysis of the aqueous plant extract of *T. crustacea* shows typical spectroscopic reaction at the wavelength of 299nm. X-ray diffraction of iron nanoparticles was observed at 2Ø values ranging from 10^0 to 80^0 shows eight major peaks which indicates the crystalline nature of iron nanoparicles. The average crystalline size of the iron nanoparticles is 5.09 nm and are also reported in the figure 3.

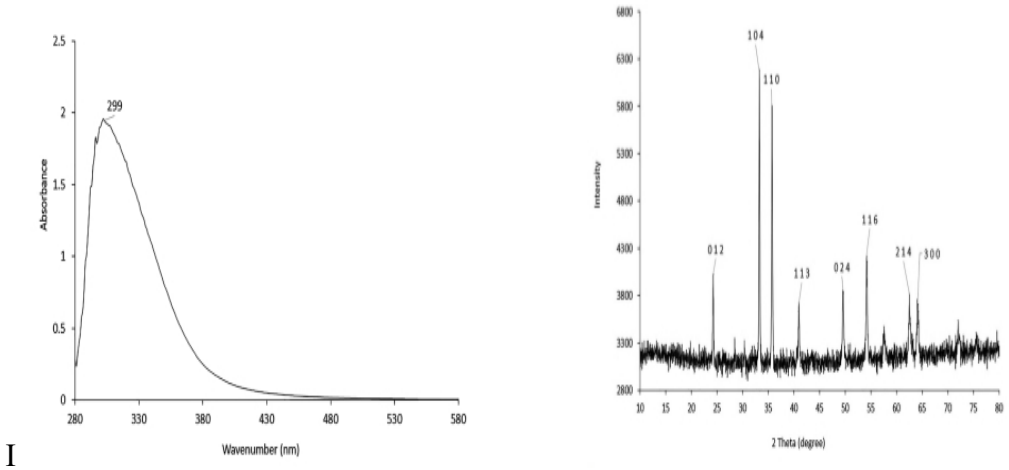

I

UV-visible spectrum **XRD spectrm**

Figure 3: Chromatogram for UV-visible and XRD spectroscopic analysis showing iron nanopaticles.

ii. FTIR analysis for iron nanoparticles of the experimental plant

FTIR analysis for iron nanoparticles of the ethanolic extract of the powdered whole plant of *T. crustacea* is used for identifying the functional groups of active components such as alkynes, alkanes, amides, misc, alkenes, carboxylic acids, aromatics and alkyl halides having the frequency range (cm^{-1}) such as 3277.40, 2922.36, 1619.99, 1431.94, 1003.57, 911.71,

633.23, 608.40, 2851.28, 2363.84, 2327.44, 1555.00, 1241.80, 796.24, 828.91, 737.68 and 667.08 cm-1 noted in the table 2 & figure 4.

Table 2: FTIR analysis of the ethanolic extract of powdered whole plant of *T. crustacea* (L.) Cham. & Schltdl. for iron nanoparticles.

SI. No.	Wave length	Functional groups	Structure
1	3277.40	Alkynes	RC#C-H
2	2922.36	Alkanes	RCH2CH3
3	1619.99	Amides	RCONH2
4	1431.94	Misc.	S=O sulphate
5	1003.57	Misc.	P-OR ester
6	911.71	Alkenes	RCH=CH2
7	633.23	Alkynes	RC#CH
8	608.40	Alkynes	RC#CH
9	2851.28	Alkanes	RCH2CH3
10	2363.84	Misc.	P-H phosphine
11	2327.44	Misc.	Si-H silane
12	1555.00	Carboxylic acids	RCO-O-
13	1241.80	Misc.	Si-CH3
14	796.24	Alkenes	R2C+CHR

15	828.91	Aromatics	Para-disub
16	737.68	Aromatics	1,2,3-trisub
17	667.08	Alkyl halides	R-Br

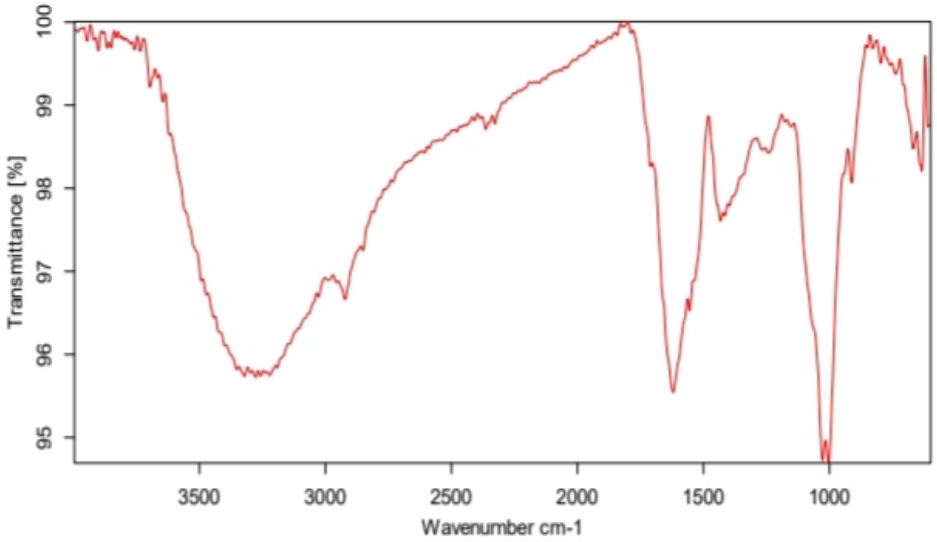

Figure 4: Chromatogram for FTIR analysis of the ethanolic extract of powdered whole plant of *T. crustacea* (L.) Cham. & Schltdl. for iron nanoparticles.

iii. SEM and TEM analysis

SEM analysis of the whole plant aqueous extract of *T. crustacea* is mostly cluster of spherical shaped iron nanoparticles. TEM images showed that the nanoparicles are spherical having non-uniform distribution and the mean size of about 16.07nm as shown in plate 2.

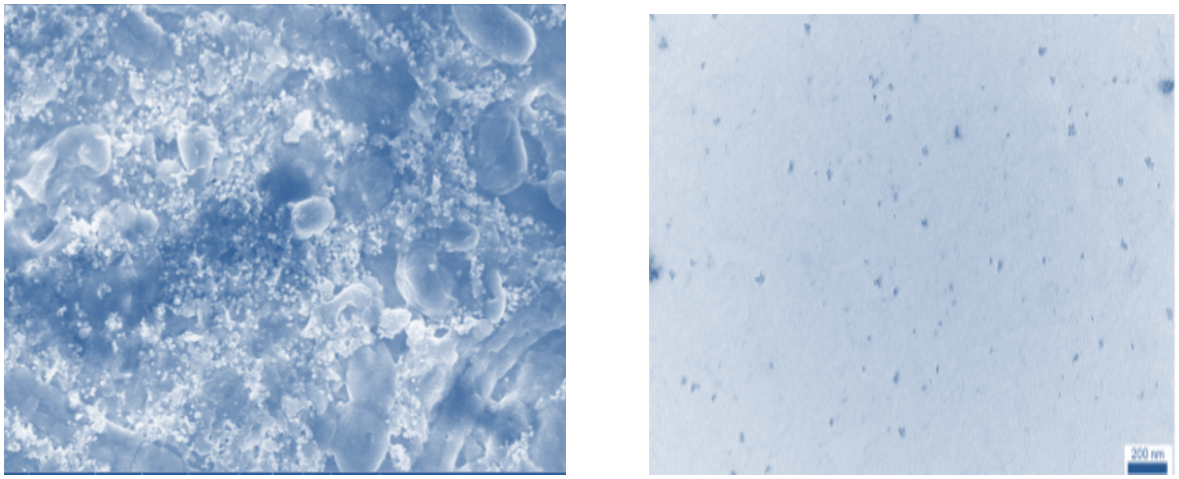

A) SEM **B) TEM**

Plate 2: SEM and TEM image showing iron nanoparticles of *T. crustacea*

Anti-microbial activity of synthesized silver and iron nanoparticles

Anti-microbial activity of the whole plant silver and iron coated extract of *T. crustacea*

was performed by using five bacterial strains such as *Escherichia coli*, *Klebsiella pneumonia*, *Bacillus subtilis*, *Staphylococcus aureus*, *Lactobacillus acidophilus* and three fungal strains such as *Aspergillus niger*, *Aspergillus flavus* and *Pencillium notatum* are shown in 3.

In silver nanoparticle coated whole plant extract shows maximum activity on *Escherichia coli* and *Staphylococcus aureus* (25mm) followed by *Pencillium notatum* (23mm); *Lactibacillus acidophilus* and *Aspergillus flavus* (20mm); *Bacillus subtilis* (18mm); *Aspergillus niger* (17mm) and *Klebsiella pneumonia* (15mm) respectively represented in the table 3 & plate 3.

The iron nanoparticle coated whole plant extract shows maximum activity on *Escherichia coli* (23mm) followed by *Staphylococcus aureus* (20mm); *Pencillium notatum* (17mm); *Klebsiella pneumonia*, *Bacillus subtilis* and *Aspergillus flavus* (15mm) and *Aspergillus niger* (9mm) respectively. Negative zone of inhibition was observed in *Lactobacillus acidophilus* against iron nanoparticles coated on experimental plant as recorded in the table 3 & plate 3.

The silver nanoparticles showed efficient anti-microbial activity as compared to iron nanoparticles. Standard drug of Streptomycin (100 µg/disc) was used as positive control and empty sterile disc was used as negative control for anti-bacterial activity and the standard drug of Fluconazole 150mg concentration was used as positive control and empty sterile disc was used as negative control for anti-fungal activity.

Table 3: Anti-microbial activity of the whole plant sample of *T. crustacea* (L.) Cham. & Schltdl. for silver & iron nanopartices.

Organisms		AgNP3	FeNP3	Positive Control	Negative Control
Bacteria	***Escherichia coli***	25	23	25	NZ
	Klebsiella pneumoniae	15	15	20	NZ
	Bacillus subtilis	18	15	23	NZ
	Staphylococcus aureus	25	20	28	NZ
	Lactobacillus acidophilus	20	NZ	26	NZ
Fungi	***Aspergillus niger***	17	9	21	NZ
	Aspergillus flavus	20	15	22	NZ
	Pencillium notatum	23	17	25	NZ

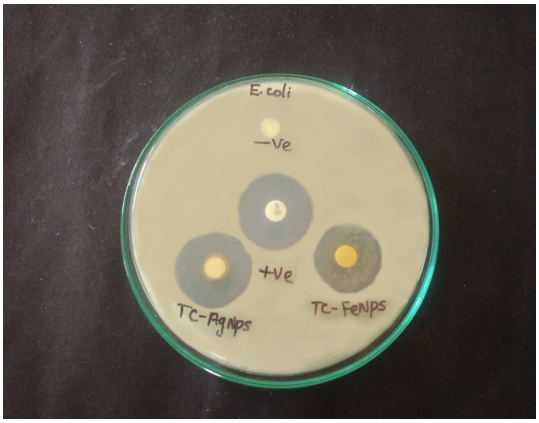

A) *E. coli*

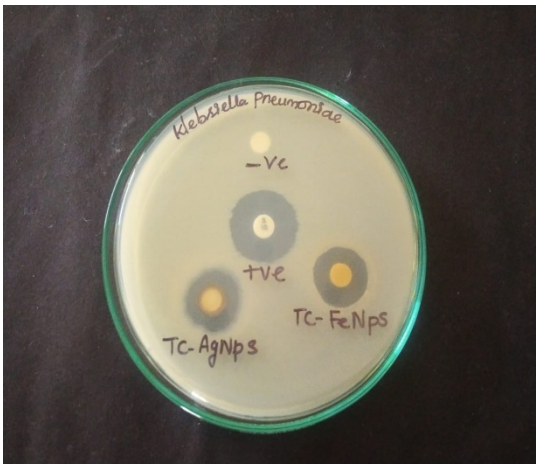

B) *Klebsiella pneumonia*

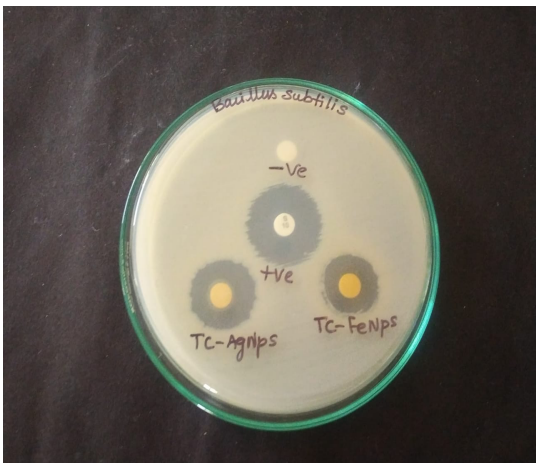

C) *Bacillus subtilis*

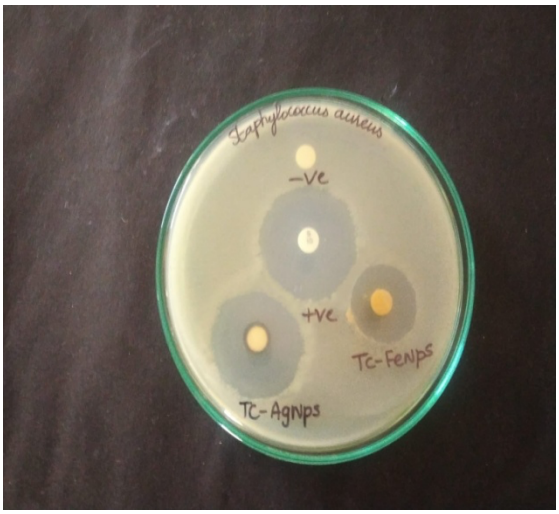

D) *Staphylococcus aureus*

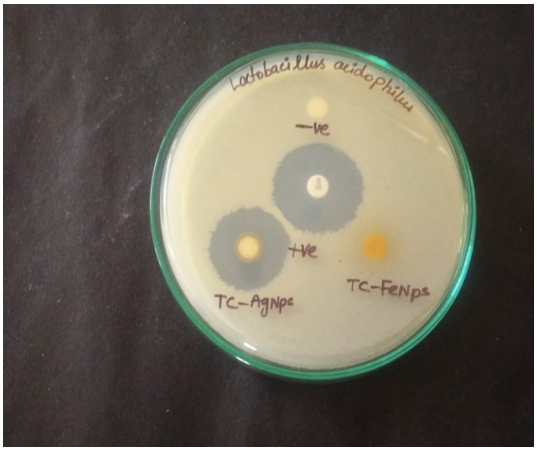

E) *Lactobacillus acidophilus*

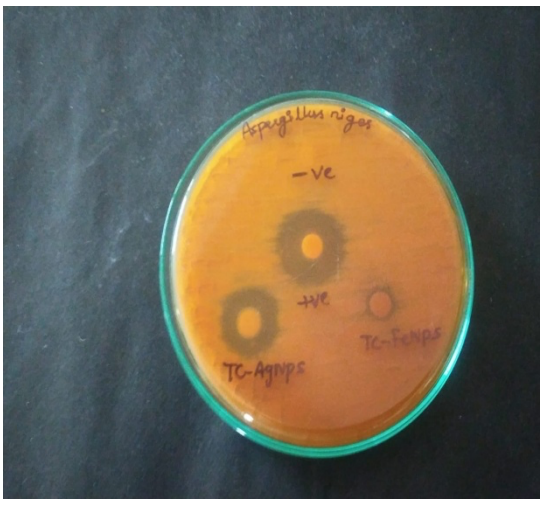

F) *Aspergillus niger*

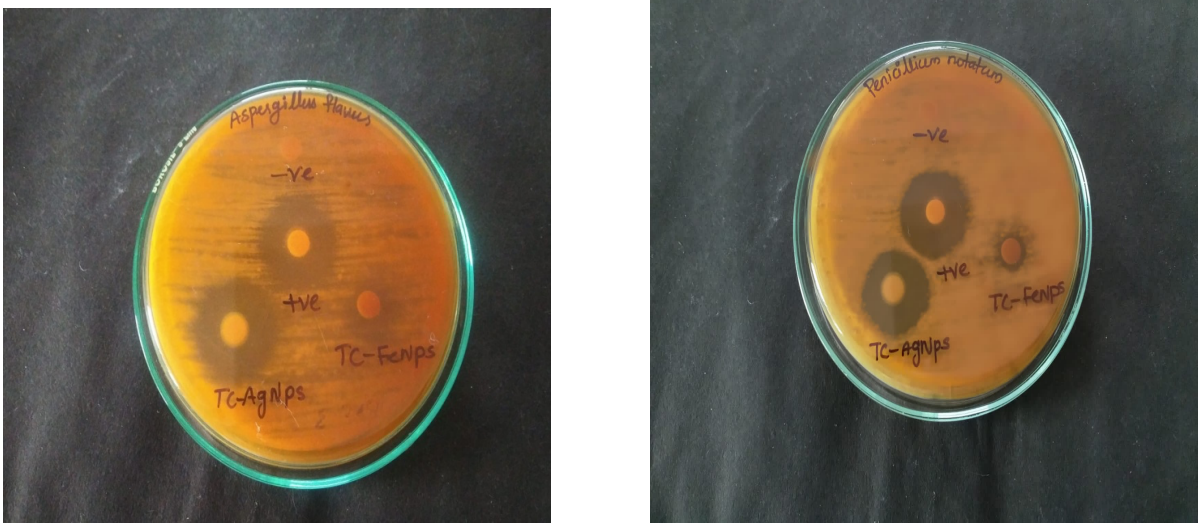

G) *Aspergillus flavus* **H) *Penicillium notatum***

Plate 3: Anti-microbial activity of the whole plant sample of *T. crustacea* (L.) Cham. & Schltdl. for silver & iron nanopartices.

Green synthesis of nanoparticles utilizes plant extracts as both reducing and capping agent eliminating the necessity of harmful agents (Peralta-Videa *et al.*, 2016). Plant extract contain various phytochemicals such as polyphenols, flavonoids, terpenoids, phenolic acids which are responsible for the reduction and formation of stabilized nanoparticles (Izadiyan *et al*., 2020).

Synthesis of nanoparticles using biological materials is gaing impetus in recent years owing to their defined chemical, optical, photo electro chemical and electronic properties (Lin *et al*., 2000). The synthesis and assembly of nanoparticles involving organisms ranging bacteria, fungi and even higher plants would benefit from the development for clean, nontoxic and environment acceptable for "green chemistry" (Bhattacharya *et al*., 2005).

The present investigation on UV-visible spectroscopic analysis of *T. crustacea* shows a typical spectroscopic reaction at the wavelength of 427 nm in which the initial pale yellow colour of the mixture changed to dark brown confirms the presence of silver nanoparticles similar result was identified in the plant leaf extract of *Clitoria ternatea* (L.) Kuntze and *Solanum nigrum* L (Narayanaswamy *et al.,* 2015). Sastry *et al*., (2003) reported that, the silver nanoparticles exhibited striking colours from light yellow to brown.

Shankar *et al.* (2003) reported the silver nanoparticles exhibited yellowish brown colour in aqueous solution due excitation of surface plasmon vibrations in silver nanoparticles. In UV-visible spectrum *T.crustacea* shows maximum absorbance peak at 427nm. XRD pattern of the siver nanoparticles shows nine major peaks and the synthesized silver nanoparticles are crystalline in nature. The observed result are in accordance with the result of Raut *et al.* (2009) where, the XRD studies revealed that, the silver nano particles are polydispersed and are ranged from 10 to 50 nm.

SEM analysis silver nanoparticles of the whole plant ethanolic extract of *T. crustacea* shows a cluster of spherical shaped silver nanoparticles with a non-uniform distribution and the TEM analysis demonstrates multi-spherical particles with a non-uniform distribution of silver nanoparticles of different sizes such as 7.98, 12.34, 11.87, 13.56 and 15.92 nm and the mean size of about 16.09 nm lies in the nano range. Savithramma *et al.* (2011)

reported that relatively spherical shaped silver nanoparticles formed with diameter ranging from 30-40 nm in *Boswellia ovalifoliolata* Roxb. ex Colebr. and 40 nm in *Shorea tumbuggaia* Roxb. The above findings are similar to those of the present investigation.

Kumar *et al*., (2012) explained that, silver nanoparticles obtained from aqueous leaf extract of *Sargassum tenerrimum* J.Agardh were fairly toxic to *Pseudomonas aeruginosa* while, they showed a moderate toxicity against *P. vulgaris, E.coli, B. subtilis* and *P. putida*. The above investigation differs from that of the present investigation. Anti-microbial activity of AgNPs prepared from *Lavandula intermedia* Grosso flower extract showed no activity and the enhancement of activity is most likely based on silver iron relased by AgNPs, destroying cells walls and secondary metabolites adsorbed on AgNPs (Elemike *et al*., 2017).

Green synthesis of AgNPs reported that *Artemisia oliveriana* J.Gay ex DC. Leaf ethanol extract or phytochemicals used in the synthesis may have some contribution to enhance the anti-microbial activities of the nanoparticles, compared to those synthesized through non-biological routes (Fard *et al*., 2018; Oliver *et al*., 2018). The anti-bacterial activity of AgNPs depends on various factors such as pH, temperature, test microorganisms, concentration, size and shape of nanoparticles (Tang & Zheng, 2018). Lia *et al*., (2020) reviewed that *Humulus lupulus* L. silver nanoparticle synthesized aqueous extract shows robust anti-microbial activity with an inhibition zone size of 9 to 26 mm. Silver has been extensively used as an anti-microbial agent for food preservation and storage for medical and therapeutic applications while, silver nanoparticles synthesized from *Allium ampelopraum* L. aqueous extract has been used as an antiseptic for treating wounds and burns (Jallian *et al*., 2020).

After reaction with $AgNO_3$ and *Conocarpus lancifolius* Engl fruit extract are shown in image spectral analysis reveals a slight shift in the spectra's peaks direction such as 620, 1070, 1250, 1485, 1560, 1620, 1735, 1860, 2360, 2800, 2950, 3570, 3650 and 3810cm^{-1} respectively were detected in the spectral pattern (Mohammad *et al.,* 2022). 653.98, 623.19, 1773.18, 1751.26, 1531.78, 759.13 and 687.49 cm^{-1}.

Plants are naturally composed of organic reducing agents, making them more suitable and adaptive for nanoparticle synthesis (Mukunthan *et al*., 2012). Several plant extracts such as *Camellia sinensis* (L.) Kuntze, *Azadirachta indica* A.Juss., *Tridax procumbens* L., *Passiflora tripartitavar* (Kunth), *Syzygium cumini* (L.), *Terminalia chebula* Retz., *Salvia officinalis* L., *Dodonaea viscose* Jacq., Oolong tea, and *Rumex acetosa* L. are reported to synthesize different types of FeNPs but specific applications Sadhasivam *et al.,* 2020).

Flower extract mediated FeNPs of *Musa ornata* Roxb. shows absorption peaks between 250 and 350 nm (Saranya *et al*., 2017). *Tridax procumbens* L. mediated synthesis of FeNPs when subjected to UV analysis, displayed the highest absorption peak at 450 nm (Kavitha *et al*., 2018). FTIR analysis of FeNPs synthesized by flower extract of *Musa ornata* Roxb. performed between the range of 400–4000 cm^{-1} shows three sharp peaks at 480.69, 3383.42, and 1634.15 cm-1 (Saranya *et al*., 2019). SEM analysis of FeNPs with a diameter of 7.7 nm synthesized by using *Passiflora foetida* L. extract (Suganya *et al*., 2016).

CONCLUSION

In this research, the whole plant extract of *T. crustacea* is considered for the production of silver and iron nanoparticles. The synthesized nanoparticles were confirmed using visual screening, UV-Vis analysis, FTIR analysis, and XRD analysis. After evaluating all of the life history traits, we concluded that green-synthesized silver and iron nanoparticles are nontoxic

in nature. Overall, they show a considerable anti-microbial potential and might be utilized as anti-microbial agents against pathogenic microbes while maintaining nontoxicity to humans.

REFERENCES

Ahmed, S, Ahmad, M, Swami, BL & Ikram, S 2016, 'A review on plant extract mediated synthesis of silver nanoparticles for anti-microbial applications: a green expertise', Journal of Advanced Research, vol. 70, no. 1, pp. 17-28.

Assam, AJP, Dzoyem, JP, Pieme, CA & Penlap, VB 2010, '*In vivo* antibacterial activity and acute toxicity studies of aqueous-methanol extract of *Sida rhombifolia* Linn. (Malvaceae)', BMC Complementary and Alternative Medicine, vol. 10, no. 40, pp. 1-7.

Austin, LA, Samera Ahmad, Bin Kang, Kathryan, Mahmoud, Mary & Mastafa, A 2014, 'Cytotoxic effects of cytoplasmic targeted and nuclear targeted gold and silver nanoparticles in HSC-3cells- A mechanistic study', Toxicology in vitro, vol. 29, no. 4, pp. 694-705.

Bauer, AW, Kirby, WM, Sherris, JC & Turck, M 1966, 'Antibiotic susceptibility testing by a standardized single disk method', Amer. I.C/in. Pathol, vol. 45, pp. 493-496.

Bhattacharya, A, Ghosal, S & Bhattacharya, SK 2005 b, 'Antioxidant effect of *Withania somnifera* glycol withanolides is chronic foot shock stress induced perturbation of oxidative free radical scavenging enzyme and lipid peroxidation in rat frontal cortex and stratum', J. Ethnopharmacol, vol. 74, pp. 1-6.

Comell Weber, Coester, C, Kreuter, J & Langer, K 2000, 'Desolvation process and surface characterization of protein nanoparticles', National Library of Medicine, vol. 194, no. 1, pp. 91-102.

Dhand, V, Soumya, L, Bharadwaj, S, Chakra, S, Deepika Bhatt & Sreedhar, B 2016, 'Green synthesis of silver nanoparticles using *Coffea arabica* seed extract and its anti-bacterial activity', National Library of Medicine, vol. 58, no.1, pp. 36-43.

Elemike, E, Damian C Onwudiwe, Anthov C Ekennia & Richard C Ehiri 2017, 'Phytosynthesis of silver nanoparticles using aqueous leaf extracts of *Lippia citriodora*: Anti-microbial, larvicidal and photocatalytic evaluations', Materials Science and Engineering, vol. 75, pp. 980-989.

Fard, NN, Noorbazargan, H, Mizrale, A, Hedayati, M, Moghimiyan, Z & Rahimi, A 2018, 'Biogenic synthesis of AgNPs using *Artemisia oliveriana* extract and their biological activities for an effective treatment of lung cancer', Artificial Cells, Nanomedicine and Biotechnology, vol. 46, pp. 1047-1058.

Izadiyan, Z, Kamyar Shameli, Mikio Miyake, Hirofumi Hara, Shaza Eva Binti Mohamad, Katayoon Kalantari & Elisa Rasouli 2020, 'Cytotoxicity assay of plant mediated synthesized iron oxide nanoparticles using *Juglans regia* green husk extract', Arabian Journal of Chemistry, vol. 13, no. 1, pp. 2011-2023.

Jallian, F, Chahardoli, A, Sadrjavadi, K, Fattahi, A & Shokoohinia, Y 2020, 'Green synthesized silver nanoparticles from *Allium am*pelopranum aqueous extract: characterization anti-oxidant activities, anti-bacterial and cytotoxicity effects', Advanced Powder Technology, vol. 31, no. 3, pp. 1323-1332.

Jeong, SH, Yeo, SY& Yi, SC 2005, 'The effect of filler particle size on anti-bacterial properties of compounded polymer/ silver fibers', Journal of Materials Science, vol.40, no. 20, pp. 5407-5411.

Kandish, M & Chandrasekaran, KN 2021, 'Green synthesis of silver nanoparticles using *Catharanthus roseus* flower extracts and the determination of their anti-oxidant, anti-microbial and photocatalytic activity', Journal of Nanotechnology, vol. 20, pp. 18.

Kohner, PC, Rosenblatt, JE & Cockerill, FR 1994, 'Comparison of agar dilution and disk diffusion testing of Ampicillin against *Haemophilus* sps by using in house and commercially prepared media', J. Clin. Microbiol, vol. 32, pp. 1594-1596.

Kumar, P, Selvi, SS, Prabha, AL & Govindaraju, M 2012, 'Synthesis of silver nanoparticles from *Sargassum* and screening phytochemical for its antibacterial ctivity', Nano Biomedicine and Engineering, vol. 4, no. 1, pp. 12-16.

Lia, R, Pana, Y, Lia, N & Chuang, W 2020, 'Anti-bacterial and cytotoxic activities of a green synthesized silver nanoparticles using corn silk aqueous extract', Colloids. Surf. A., vol. 598, pp. 12-24.

Lin, SM, Lin, PQ, Guo, HQ, Zhang, ZH & Wang, ZG 2000, 'Solid state commun', pp. 615-618.

Makarov, VV, Love, AJ, Sinitsyna, OV, Makarova, SS, Yaminsky, IV, Taliansky, ME & Kalinina, NO 2014, 'Green nanotechnologies: synthesis of metal nanoparticles using plants', Acta Naturae, vol. 6, no.1, pp.35-44.

Mathabe, MC, Nickolova, RV, Lall, N & Nyazena, NZ 2006, 'Antibacterial activities of medicinal plants used for the treatment of diarrhoea in Limpopo Province, South Africa', Journal of Ethnopharmacology, vol. 105, pp. 286-293.

Mohammad Olves, Mohd Ahmar Raul, Mohammad Aslam, Huda A Qari, Hana Sonbol, Irfan Ahmad, Gaffar Sarwar Zaman & Mohd Saeed 2022, 'Green synthesis of silver nanoparticles by Conocarpus lancifolius plant extract and their anti-microbial and anti-cancer activities', Saudi Journal of Biological Sciences, vol. 29, pp. 460-471.

Mukunthan, KS & Balaji, S 2012, 'Silver nanoparticles shoot up from the root of *Daucus carrota* L', International Journal of Green Nanotechnology, vol. 4, no.1, pp.45-67.

Narayanaswamy Krithiga, Athimoolan Rajalakshmi & Ayyavo Jayachithra 2015, 'Green synthesis of silver nanoparticles using leaf extracts of *Clitoriaternatea* and *Solanum nigrum* and study its antibacterial effect against common noscomial pathogens', Journal of Nanoscience, pp.8pgs.

Oliver, S, Weigh, H, Liang, Y, Yang, S & Boyer, C 2018, 'Enhancing the anti-microbial and antibiofilm effectiveness of silver nanoparticles prepared by green synthesis', Journal of Materials Chemistry, vol. 6, no. 24, pp. 4124-4138.

Peralta-Videa, JR, Yuxiong Huang, Parsons, JG, Lijuan Zhao, Laura Lopez Moreno, Hernandez-Viezcas, JA & Gardea-Torresdey, JL 2016, 'Plant based green synthesis of metallic nanoparticles: scientific curiosity or a realistic alternative to chemical synthesis', Nanotechnology for Environmental Engineering, vol. 1, no. 4, pp.456-478.

Raut Rajesh, W, Lakkakula Jaya, S, Kolekar Niranian, D & Mendhulkar Vijay, B 2009, 'Photosynthesis of silver nanoparticles using *Gliricidia sepium* (Jacq.)', Curr. Nanosci, vol. 5, no. 1, pp. 117-122.

Rodrigues, AG, Liu Yu Ping, Marcato, PD, Alves, OL, Silva, MCP, Ruiz, RC, Melo, IS, Tasic, L & Souza, AOD 2013, 'Biogenic antimicrobial silver nanoparticles', Applied Microbial and Cell Physiology, vol. 5, no. 3, pp. 234-243.

Sadhasivam, S, Shanmugam, M, Umamaheshwaran, PD, Venkattappan, A & Shanmugam, A 2020, 'Zinc oxide nanoparticles: Green synthesis and Biomedical applications', Jounal of Cluster Science, vol. 32, no. 3, pp. 1441-1445.

Sahayaraj, K, Rajesh, S & Rathi, JM 2012, 'Silver nanoparticles biosynthesis using marine algae *Padina pavonica* (Linn.) and its microbial activity', Digest Journal of Nanomaterials and Biostructures, vol. 7, no. 4, pp. 1557-1567.

Salari, S, Bahabadi, SE, Samzadeh-Kermani, A & Yosefzaei, F 2018, '*In vitro* evaluation of anti-oxidant and anti-bacterial potential of green synthesized silver nanoparticles using *Prosopis farcta* fruit extract', Iranian Journal of Pharmaceutical Research, vol. 25, no.14, pp. 1-24.

Sastry, M, Ahmed, A, Khan, MI & Kumar, R 2003, 'Biosynthesis of metal nanoparticles using fungi and actinomycetes', Current Science, vol. 85, no. 2, pp. 202-206.

Savithramma, N, Linga, M & Suvarnalatha Devi, P 2011, 'Evaluation of antibacterial efficacy of biologically synthesized silver nanop[articles using stem barks of *Bowsellia ovalifoliolata* and *Shorea tumbuggaia'*, Journal of Biological Sciences, vol. 11, no. 1, pp. 39-45.

Shanker, SS, Ahmad, A, Pasricha, R & Sastry, M 2003, 'Bioreduction of chloaurate ion by *Geranium* leaves and its endophytic fungus yields gold nanoparticles of different shapes', Journal of Materials Chemistry, vol. 13, no. 7, pp. 1822-1826.

Suganya, D, Ramakritinan, CM & Rajan, MR 2016, 'Adverse effects of genotoxicity, bioaccumulation and ionoregulatory modulation of two different synthesized iron oxide nanoparticles of *Danio rerio*', Journal of Inorganic and Organomettalic Polymers and Materials, vol. 45, no. 3, pp. 56-65.

Tang, S & Zheng, J 2018, 'Anti-bacterial activity of silver nanoparticles: structural effects', Advanced Healthcare Materials, vol. 7, no. 13, pp. 170-173.

Thiyagarajan, K, Bharti, VK, Tyagi, S, Tyagi, PK, Ahuja, A, Kumar, K, Raj, T & Kumar, B , 'Synthesis of non-toxic, biocompatible, and colloidal stable silver nanoparticle using egg-white protein as capping and reducing agents for sustainable antibacterial application', RSC Advances, vol. 8, no. 41, pp. 23213–23229.

Umoren, SA, Obot, IB, & Gasem, ZM 2014, 'Green synthesis of silver nanoparticles using apple (*Malus domestica*) fruit extract at room temperature.', Journal of Materials and Environmental Science, vol. 5, pp. 907-914.

Vidya Sagar, PSR, Dharmasoth Ramadevi, Keloth Basavaiah & Sathish Mohan Botsa 2023, 'Green synthesis of siver nanoparticles using aqueous leaf extract of *Saussurea obvallata* for efficient catalytic reduction of nitrophenol, anti-oxidant and anti-microbial activity', Water Science and Engineering, vol. 17, no. 3, pp. 274-282.

Vinod Kumar, Davender Singh & Bijendaer Singh 2024, 'Mycogenic synthesis of iron nanoparticles using thermophilic mould *Myceliophthora thermophila* and their applicability in environmental remediation', Biocatalysis and Agricultural Biotechnology, vol. 56, no. 5, pp. 103-120.